THE ASTROPHYSICAL JOURNAL, 386:222–228, 1992 February 10

KNOTS IN STELLAR JETS FROM TIME-DEPENDENT SOURCES

A. C. RAGA AND LEV KOFMAN[1]
Canadian Institute for Theoretical Astrophysics, 60 St. George Street, Toronto, Ontario, Canada M5S 1A1
Received 1991 June 25; accepted 1991 August 15

ABSTRACT

We present an analytical model that describes the time-evolution of a highly supersonic jet of small opening angle ejected from a time-dependent source. With this model, we explore the possibility that the aligned knots observed along astrophysical (and in particular, stellar) jets might be the result of "internal working surfaces" produced in the jet flow as a result of a time-dependent ejection velocity.

This model allows us to carry out very concrete predictions of the shock velocities, Hα luminosities and characteristic masses of the knots in a stellar jet. We present a comparison between these predictions and previously existing observations of the HH 34 outflow (which has a very well defined, jetlike structure), and find a surprisingly good agreement between theoretical predictions and observations.

Subject headings: ISM: jets and outflows — shock waves — stars: pre–main-sequence

1. INTRODUCTION

Both extragalactic and stellar jets many times show structures of more or less regularly spaced, well aligned knots, extending away from the outflow source. These knots have been interpreted as being a result of either recollimation shocks or internal shocks formed by instabilities in the jet/environment boundary (see, e.g., the recent book on astrophysical jets of Hughes 1991).

An alternative possibility was proposed by Rees (1978), who suggested that a time-variability in the outflow source could result in the formation of shock waves travelling along the jet flow. These shock waves would produce excitation and compression in the gas, which could be identified with the knots observed in astrophysical jets.

The numerical simulations of Wilson (1984) show that supersonic variations in the source velocity result in the formation of two-shock "internal working surfaces" that travel down the jet flow. Such a model can be used to explain the intensity and velocity structure of jets that show more than one "head" (e.g., HH 46/47, Reipurth 1989; Hartigan, Raymond, & Meaburn 1990; Raga et al. 1990). Also, the structures of knots in stellar and extragalactic jets could in principle correspond to a series of such internal working surfaces travelling away from the source. In a recent paper (Kofman & Raga 1991) we have explored this possibility and we have constructed an analytical formalism (based on solutions to the viscous Burgers' equation) for describing the global structure of jets ejected from time-dependent sources. In the present paper, we extend our formalism to treat the case of jets with variable densities (Kofman & Raga 1991 studied the idealized case of a constant density flow).

Based on our simple theory, we also obtain predictions of observable quantities (e.g., the emission line intensities of the knots) and carry out a direct comparison with observations of stellar jets. In particular, for our comparison we have chosen the parameters derived from observations of the HH 34 outflow, which has one of the most striking jetlike structures found in any of the known Herbig-Haro (HH) objects (see, e.g., the reviews of Mundt 1986; Reipurth 1989). The parameters derived from observations of this stellar jet are discussed in § 2. In § 3, we derive the equations for a variable density jet ejected from a time-dependent source, and in the following sections we show the predictions and implications of our model for the physical parameters found in stellar jets.

2. PARAMETERS FOR THE HH 34 JET

In this section, we discuss the physical parameters that can be derived from the quite extensive observations of the HH 34 outflow that have been carried out in the past. In the rest of this paper we will then focus on these parameters in order to show the properties and implications of our theoretical model.

The HH 34 system shows a chain of very well aligned knots close to the source. We will call this chain of knots (which points approximately northwards, towards HH 34 itself) the "HH 34 jet." This jet is observed to have six bright knots, which have been labeled B through G by Reipurth et al. (1986). Also, several fainter knots have been discovered by Bührke, Mundt, & Ray (1988). However, we will concentrate exclusively on the brighter knots (B through G; Reipurth et al. 1986), which have intensities larger by factors of $\sim$5–10 than the fainter knots discovered later (Bührke et al. 1988).

The HH 34 jet shows a very low excitation spectrum, with [O I] 6300/Hα and [S II] (6717+31)/Hα line ratios substantially greater than unity. As Brugel, Böhm, & Mannery (1981) have shown, low-excitation HH spectra indicate that the emitting gas has a temperature not in excess of $\sim 10^4$ K, and a low ionization fraction (of order 10%). Because of this, as a rough estimate we will consider that the emitting regions in the HH 34 jet have a temperature $T \approx 10^4$ K, and an ionization fraction such that $\xi \equiv n/n_e \approx 10$ (where n_e is the electron, and n the ion + atom + electron number density).

Bührke et al. (1988) have derived electon densities $\sim$600–1000 cm^{-3} for the brighter knots of the HH 34 jet (from the density sensitive [S II] 6731/[S II] 6717 line ratio). We will choose $n_e \approx 1000$ cm^{-3} as the typical electron density of the emitting regions of the HH 34 jet.

The bright knots (B through G) of the HH 34 jet have radial velocities of $\sim$80 km s^{-1} (Reipurth et al. 1986; Bührke et al. 1988), and proper motions of $\sim$200 km s^{-1} (Reipurth 1989). From this, we derive an angle of 22° between the outflow axis

[1] On leave of absence from: Institute of Astrophysics and Atmospheric Physics, Tartu, Estonia, 202444 USSR.

and the plane of the sky. In other words, the outflow is almost on the plane of the sky, so that we can adopt a spatial velocity $v \approx 200 \text{ km s}^{-1}$ for the knots of the HH 34 jet.

The knots B through G are at positions ranging from roughly 10″ to 26″ from the source, corresponding to distances $\sim(0.7\text{–}1.9) \times 10^{17}$ cm (adopting the orientation angle derived above, and a distance of 450 pc to the HH 34 outflow). The consecutive knots in the HH 34 jet show angular separations of roughly 2″–4″, corresponding to spatial separations of $(1.5\text{–}3) \times 10^{16}$ cm. In the following we will adopt $x = 1.5 \times 10^{17}$ cm and $\Delta x = 2 \times 10^{16}$ cm as typical values for the distance from the source and the knot separation (respectively) for the bright knots of the HH 34 jet.

The remaining parameter that is necessary for a comparison with our theoretical model (described below) is the jet radius. Even though the radius is only barely resolved, Raga & Mateo (1988) and Bührke et al. (1988) have independently derived (using different deconvolution methods) a radius of $\approx 0\overset{''}{.}35$ for the brighter regions of the HH 34 jet (corresponding to $\approx 2.4 \times 10^{15}$ cm at the distance of HH 34). We therefore adopt a jet radius $r_{\text{jet}} = 2 \times 10^{15}$ cm for our comparison with the theoretical model.

3. EQUATIONS FOR A JET FROM A TIME-DEPENDENT SOURCE

3.1. *Global Structure of the Jet*

Rees (1978) first proposed that the structures of knots observed in astrophysical jets might be the result of a time-variability of the source. The numerical simulations of Wilson (1984) show that supersonic perturbations in the outflow velocity (at the injection point of the jet) result in the production of two-shock "internal working surfaces" which move down the jet flow (see also Raga et al. 1990). We present a schematic diagram of such an internal working surface in Figure 1.

A jet from a source with an extended time-dependent history (e.g., with a number of "outflow events") will have several internal working surfaces, which would be identified with the emitting knots observed along an astrophysical jet. The knots of the jet would be separated by regions of continuous flow (Wilson 1984; Kofman & Raga 1991). A schematic diagram of this configuration is shown in Figure 2. We first present a solution for the flow in the continuous regions of the flow (§§ 3.2 and 3.3) and then derive the equation of motion for the knots.

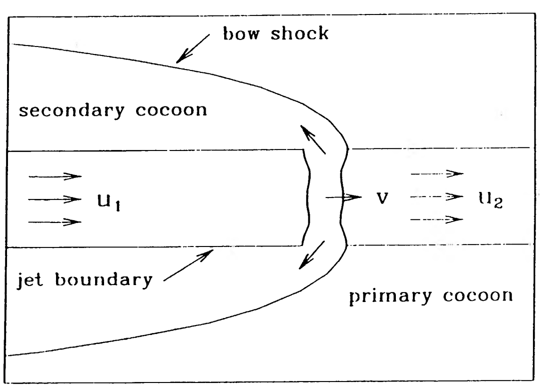

FIG. 1.—Schematic diagram showing the structure of an internal working surface in a jet flow. A two-shock structure is formed as the faster, upstream material (of velocity u_1) catches up with the slower, downstream material (of velocity u_2). The gas trapped in between the two shocks is ejected sideways by the on-axis overpressure (resulting from the compression in the shocks), forming a "cocoon" (possibly of cool gas, see the text) with a possibly very complex structure around the jet. This diagram has been taken from Raga et al. (1990).

3.2. *Free-Streaming Solution*

We assume that we have a jet with a small opening angle (i.e., with a slowly varying cross section), so that the motion occurs mainly along the symmetry axis. For such a jet, the flow can be described with the one-dimensional equation of motion:

$$\frac{\partial u}{\partial t} + u\frac{\partial u}{\partial x} + \frac{1}{\rho}\frac{\partial P}{\partial x} = 0\,, \tag{1}$$

where t is the time, x and u are the distance and velocity (respectively) along the symmetry axis, and P is the pressure.

For a highly supersonic flow, the term in equation (1) involving the pressure is negligible. In this way, see that the total derivative of the flow velocity u (following a fluid parcel) is $du/dt = 0$. In other words, in the absence of pressure forces, parcels ejected at a time τ with a velocity $u_0(\tau)$ preserve this velocity as they move away from the source. This is the "free-streaming" solution:

$$u(x, t) = u_0(\tau) = \frac{x}{t - \tau}\,, \tag{2}$$

where $u_0(\tau)$ is the velocity with which the parcel at position x and time t was ejected from the source. As discussed by Kofman & Raga (1991), in jets from time-dependent sources a number of internal working surfaces are in principle formed (one for each "pulse" of the outflow). Most of the material from each pulse ends up being "swallowed" (and then ejected sideways see Fig. 1) by the working surfaces. Because of this, at large distances from the source the continuous flow between two successive knots is formed by fluid parcels that were ejected from the source in a narrow time-interval around a time τ_n (for the nth pulse of the time-dependent jet source). From equation (2), we see that the continuous flow segment coming from the nth pulse (see Fig. 2) then degenerates into

$$u(x, t) = \frac{x}{t - \tau_n}\,, \tag{3}$$

or, in other words, for any given time the flow velocity increases linearly with distance from the source. This asymptotic solution has been described in detail by Kofman & Raga (1991).

Because of the fact that we have neglected the pressure forces, the density of the flow does not appear in our solution for the flow velocity (eq. [3]). However, the motion of the internal working surfaces does depend on the time- and position-dependent density of the flow. Because of this, in the following section we discuss an analytic solution for the density of a free-streaming flow.

3.3. *Continuity Equation*

For the sake of simplicity, we assume that the jet cross section σ has a power-law dependence on distance x from the source:

$$\sigma(x) = \sigma_0\left(\frac{x_0}{x + x_0}\right)^p\,. \tag{4}$$

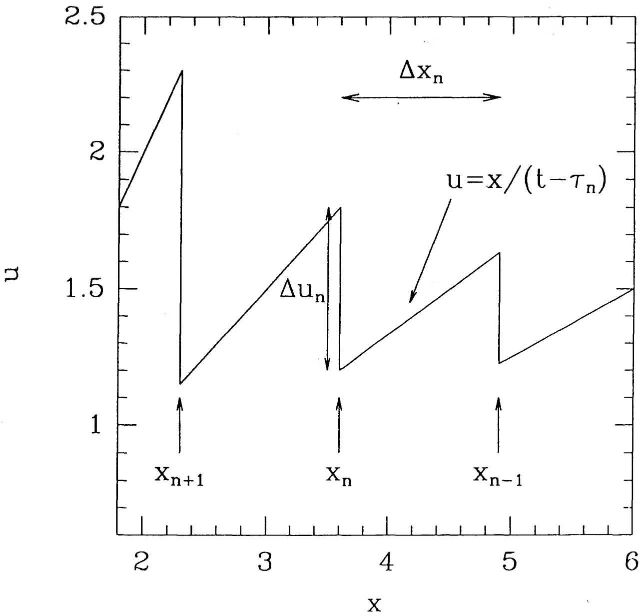

FIG. 2.—Schematic diagram showing the structure of successive working surfaces formed by a jet source with a time-dependent outflow velocity. The vertical segments of the velocity versus position curve correspond to the working surfaces (which on principle have a two-shock structure, but are treated as single discontinuities in our simplified formalism). The oblique, continuous segments (which at large distances from the source degenerate into straight lines, see the text) correspond to the gas ejected during the consecutive "pulses" of the source (which we have numbered $n-1$, n and $n+1$ in this diagram). This figure has been taken from Kofman & Raga (1991).

For example, for the case of a jet with a constant (half) opening angle α, we would have $p = 2$, $\tan\alpha = \sqrt{(\sigma_0/\pi)}/x_0$, and x would be the spherical radius. The Lagrangean continuity equation is then

$$\frac{d\rho}{dt} + \frac{\rho}{(x+x_0)^p}\frac{\partial}{\partial x}[u(x+x_0)^p] = 0\,. \tag{5}$$

If the flow field $u(x, t)$ is determined by the free-streaming condition (eq. [2]), the continuity equation (5) has the general solution

$$\rho(x, t) = \rho_0(\tau)\left(\frac{x_0}{x+x_0}\right)^p\left[1-(t-\tau)\frac{d\ln u_0}{d\tau}\right]^{-1}. \tag{6}$$

In the limit of large distances from the source this equation becomes

$$\rho_n(x, t) \approx a_n\left(\frac{x_0}{x+x_0}\right)^p\left(\frac{1}{t-\tau_n}\right), \tag{7}$$

for the continuous segment of the flow arising from the nth pulse of the source. The constant a_n is given by

$$a_n = \rho_0(\tau_n)\Big/\left|\frac{d\ln u_0}{d\tau}\right|_{\tau_n} \equiv \frac{m_n}{\sigma_0 u_0(\tau_n)}\,. \tag{8}$$

The characteristic mass m_n of the nth pulse of the source is defined as

$$m_n \equiv \sigma_0\rho_0(\tau_n)u_0(\tau_n)\tau_d\,, \tag{9}$$

where σ_0 is the initial cross section of the jet (which we assume to be independent of time), $u_0(\tau_n)$ and $\rho_0(\tau_n)$ are the velocity and density (respectively) of the outflow at the injection point, and

$$\tau_d = \left[\left|\frac{d\ln u_0}{d\tau}\right|_{\tau_n}\right]^{-1} \tag{10}$$

is the characteristic decay time scale of the nth pulse. In principle, m_n is of the same order of magnitude as the total mass M_n ejected in the pulse. However, the precise relationship between m_n and M_n depends on the details of the time-dependent velocity and density of the ejection event. From equations (7) and (8), we then finally obtain

$$\rho_n(x, t) = \left[\frac{m_n}{\sigma_0 u_0(\tau_n)}\right]\left(\frac{x_0}{x+x_0}\right)^p\left(\frac{1}{t-\tau_n}\right). \tag{11}$$

In the following section, we will use the density and velocity fields derived above in order to derive the motion of the internal working surfaces of the jet.

3.4. *The Motion of the Knots*

In the previous two sections, we have derived the velocity and density profiles of the continuous segments of the jet flow for the asymptotic regime of large distances from the source. These solutions can be used in order to obtain an equation of motion for the internal working surfaces of the flow.

As discussed by Raga et al. (1990), the motion of an internal working surface can be derived by considering a coordinate system moving with the velocity v_s of the working surface. In this coordinate system, we have a balance between the pre- and post-working surface ram pressures: $\rho_1 v_1^2 = \rho_2 v_2^2$ (where v is the flow velocity measured in this particular frame of reference, and the subscripts 1 and 2 indicate the values upstream and downstream of the working surfaces, see Fig. 1). Transforming the velocities back to a coordinate system fixed on the source of the jet, we obtain the differential equation (see Raga et al. 1990)

$$v_s = \frac{dx_s}{dt} = \frac{u_1+\beta u_2}{1+\beta}\,, \tag{12}$$

where

$$\beta = \sqrt{\frac{\rho_2}{\rho_1}}\,. \tag{13}$$

The value of β can be determined from our solution for the density field (eq. [11]):

$$\beta = \sqrt{\frac{a_2(t-\tau_1)}{a_1(t-\tau_2)}} \xrightarrow[t \gg |\tau_2-\tau_1|]{} \sqrt{\frac{a_2}{a_1}}\,. \tag{14}$$

In other words, in the asymptotic regime of large distances from the source (which also can be characterized by the condition $t \gg |\tau_2 - \tau_1|$) the value of β is constant, and equal to the square root of the initial density ratio of the two consecutive pulses (inversely weighted with the corresponding decay time scales, see eqs. [8] and [14]) that gave rise to the working surface.

For a constant value of β (see eq. [14]), equation (12) can be directly integrated to obtain

$$x_s(t) = C[(t-\tau_1)(t-\tau_2)^\beta]^{1/(1+\beta)} \approx C\left(t - \frac{\tau_1+\beta\tau_2}{1+\beta}\right), \tag{15}$$

where for the second equality we have again explicitly considered the limit of large distances from the source. The quantity C is an integration constant which is equal to the (constant) velocity v_s of the working surface: from equation (15), we have

$$v_s = \frac{dx_s}{dt} = C . \tag{16}$$

Furthermore, if we use equations (2) and (12) we obtain

$$v_s = C = \frac{u_0(\tau_1) + \beta u_0(\tau_2)}{1 + \beta} . \tag{17}$$

From this, we conclude that at large distances from the source, the internal working surfaces move with a constant velocity v_s (see eq. [17]), which is determined by the velocity and density profiles of the pairs of ejection events which lead to the formation of the respective working surfaces. This result is a generalization of the work of Kofman & Raga (1991, who studied the case of a constant density jet) to the case of jets with variable densities.

4. THE SHOCK VELOCITIES

The asymptotic solution described in the previous section can be used to derive the strength of the shock waves associated with the internal working surfaces. This has already been done by Kofman & Raga (1991) for the case of a constant density jet.

The velocity jump Δu is equal to $u_2(x_s, t) - u_1(x_s, t)$, where the indices 1 and 2 indicate the material downstream and upstream of the working surface. For the limit of large distances from the source, we can use equation (3) to obtain

$$\Delta u = \left(\frac{x_s}{t - \tau_2}\right) - \left(\frac{x_s}{t - \tau_1}\right) \approx \frac{v_s^2 \Delta\tau}{x_s} , \tag{18}$$

where $\Delta\tau = \tau_2 - \tau_1$ is the time interval separating the two outflow events that gave rise to the working surface, and for the second equality we have also used equations (15) and (16). From the ram pressure balance condition (eq. [12]) and the density field (eq. [7]), we can obtain the shock velocities v_1 and v_2 (i.e., the velocities of the upstream and downstream flow measured in a frame of reference moving with the working surface)

$$v_{1,2} = f_{1,2}\, \Delta u = f_{1,2}\, \frac{v_s^2 \Delta\tau}{x_s} , \tag{19}$$

where

$$f_{1,2} = \frac{\sqrt{a_1 a_2} - a_{2,1}}{a_{1,2} - a_{2,1}} . \tag{20}$$

We should note that for the case of a jet from a periodically varying source, this result provides a very strong prediction that in principle could be observationally tested. For a periodic source, we have $f_1 = f_2 = \frac{1}{2}$ (see eqs. [8] and [20]), so that $v_1 = v_2 = \Delta u/2$ (eq. [19]). Also, for this "periodic jet," all of the internal working surfaces should move with the same velocity v_s (eq. [17]). The value of $\Delta\tau = \tau_2 - \tau_1$ (which in this case is equal to the period of oscillation of the source) can then be calculated directly from the observations of a stellar jet as

$$\Delta\tau = \frac{\Delta x_s}{v_s} , \tag{21}$$

where Δx_s is the spatial separation between two successive knots of the jet. Our model predicts that for the successive knots along the jet, the shock velocity (associated with the working surfaces) should decrease inversely proportional to the distance x_s from the source (see eq. [19]).

For the parameters appropriate fo HH 34 (see § 2), we obtain $\Delta\tau \approx$ 20–40 yr (from eq. [21]), and (from eqs. [18] and [19]) $v_{\rm shock} \approx$ 10–20 km s^{-1}. In other words, if the knots of the HH 34 jet are indeed working surfaces formed from a quasi-periodic source variability, the shock velocities associated with the knots should be very low. This is in apparent qualitative agreement with observations of HH 34, which show that this object has a very low excitation spectrum (see § 2).

These low values ($\sim$10–20 km s^{-1}) for the shock velocity raise the following question about our models. For determining the motion of the knots, we have considered a simple ram pressure balance across an internal working surface (see § 3.4), in which we have neglected the preshock thermal pressures. Put in another way, if the temperature of the continuous, free-streaming interknot regions (see § 3.2) were $\sim 10^4$ K, the sound speed would be lower but comparable to the shock velocities deduced for HH 34, so that the preshock thermal pressure would not be negligible.

However, while the postshock region (i.e., the gas "trapped" between the shock pairs of the working surfaces, see Fig. 1) does have a temperature $\sim 10^4$ K, the preshock interknot regions are in principle very cold. Even if the jets were ejected with a high initial temperature, at large distances from the source the temperature would be low as a result of both radiative and adiabatic cooling. The adiabatic cooling is a direct consequence of the "stretching" of the flow that results from the time-dependence of the ejection velocity (see § 3.3). In this way, we expect that at large distances from the source the interknot regions will be very cold. Because of this, our simplified equation of motion for the knots (in which the preshock pressure has been neglected, see above and § 3.4) should be valid, even for the low $\sim$10–20 km s^{-1} shock velocities deduced for the HH 34 jet.

5. THE LINE INTENSITIES

We now have the shock velocities (§ 4) associated with the internal working surfaces of the jet. Also, we have found a solution for the density field (§ 3.3), which allows us to calculate the preshock density for both the forward and backward facing shocks of the working surfaces (see Fig. 1). If we assume that these shocks (and the recombination regions behind them) can be described in an approximate way with one-dimensional shock wave models, we can use the predictions of line fluxes from one-dimensional shock models in order to determine the emission of the working surfaces. For this approximation to be valid, the cooling distance behind the shocks should be smaller than the jet radius (the validity of this assumption is discussed in more detail in § 8).

From the line fluxes predicted by Hartigan, Raymond, & Hartmann (1987), we find that the Hα intensity (per unit area of a plane-parallel shock front) is quite accurately described by the interpolation formula

$$I_{\rm H\alpha} = \epsilon \rho_{\rm ps} v_{\rm shock}^{\kappa} , \tag{22}$$

where $\rho_{\rm ps}$ is the preshock density, and $v_{\rm shock}$ is the shock velocity. From a fit to the "equilibrium preionization" models of Hartigan et al. (1987) in the $v_{\rm shock}$ = 20–80 km s^{-1} velocity range, we obtain $\kappa = 3.8$, and $\epsilon = 3.21 \times 10^{11}$ ergs cm s^{-1} g^{-1} (km s^{-1})$^{-3.8}$.

The Hα luminosity of a working surface is then given by

$$L_{\mathrm{H}\alpha} = \epsilon(\rho_1 v_1^\kappa + \rho_2 v_2^\kappa)\sigma\ , \tag{23}$$

where σ is the cross section of the jet (eq. [4]), and we have added together the contributions from the forward- and the backward-facing shocks of the working surface. Using equation (19) for the shock velocities v_1 and v_2 and equation (8) (which gives the values of the constants $a_{1,2}$ as a function of the characteristic masses $m_{1,2}$ of the pulses) we obtain

$$L_{\mathrm{H}\alpha} = \frac{\epsilon v_s^{2\kappa}(\Delta\tau)^\kappa}{x_s^{\kappa+1}}\,(m_1 f_1^\kappa + m_2 f_2^\kappa)\ . \tag{24}$$

For the case of a jet ejected from a source with a periodically varying velocity, $f_1 = f_2 = \frac{1}{2}$ (see § 4), and $m_1 = m_2 \equiv m$ (the characteristic mass of the pulses from the source, see § 3.3). The Hα luminosity of the successive working surfaces is then

$$L_{\mathrm{H}\alpha} = \frac{\epsilon v_s^{2\kappa}(\Delta\tau)^\kappa}{2^{\kappa-1}x_s^{\kappa+1}}\,m\ . \tag{25}$$

In other words, the Hα luminosity of the successive working surfaces should fall off as $x_s^{-4.8}$ with distance x_s from the source.

In Figure 3, we show the (relative) Hα luminosities of the knots of the HH 34 jet (integrated both along and across the jet for each knot) as a function of distance from the source (obtained from the observations of Raga & Mateo 1988). It is clear that at large distances from the source (where our asymptotic solution should be valid), the intensities of the knots do approximately satisfy an $x^{-4.8}$ dependence. From this we conclude that the intensity decay (at large distances from the source) of the HH 34 jet is indeed consistent with what one would expect from a model of knots produced by quasi-periodic variations in the source velocity.

6. THE ELECTRON DENSITY MEASURED IN THE WORKING SURFACES

Let us now attempt to derive an estimate of the electron density n_e in the recombination regions of the working surface

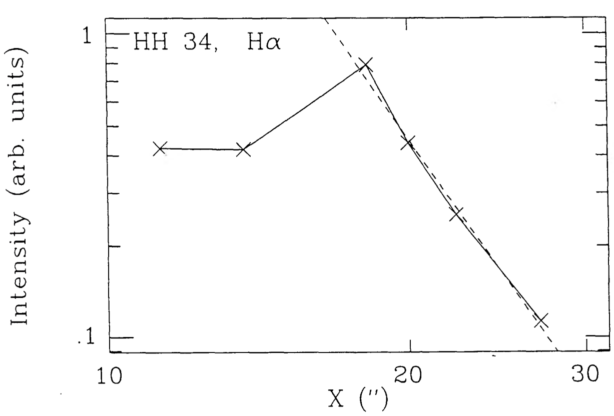

FIG. 3.—Hα intensities for the bright knots of the HH 34 jet (B through G, using the nomenclature of Reipurth et al. 1986) as a function of distance x_s between the source and the successive knots. The intensities are given in arbitrary units, and have been taken from Raga & Mateo (1988). The dashed line represents an Intensity $\propto x_s^{-4.8}$ dependence, which seems to be consistent (at least in a qualitative way) with the intensity decay of the HH 34 jet at large distances from the outflow source.

shocks. Even though with our simple formalism it is only possible to derive a crude estimate, it is a highly interesting prediction because it can be directly compared with observational determinations of n_e (from the density sensitive [S II] 6731/[S II] 6717 line ratio, see § 2) in stellar jets.

The on-axis gas pressure in between the two shocks of a working surface is given by

$$P = \xi n_e kT = \rho_{1,2} v_{1,2}^2\ , \tag{26}$$

where $\xi = n/n_e$ (n is the total, ion + atom + electron number density), and the preshock densities ρ_1, ρ_2, and shock velocities v_1, v_2 have been defined in § 4. If we could empirically determine n_e, ξ and T, we could obtain the preshock densities as

$$\rho_{1,2} = \frac{\xi n_e kT}{f_{1,2}^2 v_s^4 \Delta\tau^2}\,x_s^2\ , \tag{27}$$

where we have used equations (19) and (26).

We can also use the empirically determined electron density in order to determine the characteristic masses $m_{1,2}$ (of the two outflow events that have given rise to the observed working surface). From equations (3), (7), (8) and (27), we obtain

$$m_{1,2} = \frac{\sigma\xi n_e kT x_s^3}{f_{1,2}^2 v_s^4 \Delta\tau^2}\ . \tag{28}$$

For the case of a periodically varying source, this equation reduces to

$$\begin{aligned} m = \frac{4\pi r_{\mathrm{jet}}^2 \xi n_e kT x_s^3}{v_s^4 \Delta\tau^2} &= 7.35 \times 10^{-6}\ M_\odot \\ &\times \left(\frac{r_{\mathrm{jet}}}{2\times 10^{15}\ \mathrm{cm}}\right)^2 \left(\frac{\xi}{10}\right)\left(\frac{n_e}{1000\ \mathrm{cm}^{-3}}\right)\left(\frac{T}{10^4\ \mathrm{K}}\right) \\ &\times \left(\frac{x_s}{1.5\times 10^{17}\ \mathrm{cm}}\right)^3 \left(\frac{200\ \mathrm{km\ s}^{-1}}{v_s}\right)^4 \left(\frac{30\ \mathrm{yr}}{\Delta\tau}\right)^2\ , \end{aligned} \tag{29}$$

where we have calculated the cross section as $\sigma = \pi r_{\mathrm{jet}}^2$ (r_{jet} = the cylindrical radius of the jet at position x_s), and for the second equality we have normalized the equation to the parameters relevant for the HH 34 jet (which we have defined in § 2). From this, we would conclude that the ejection events which lead to the formation of the knots had characteristic masses of the order of $10^{-5}\ M_\odot$. For the chain of five bright knots of the HH 34 jet, we would then estimate a total mass of $\sim 5 \times 10^{-5}\ M_\odot$. We can also estimate the mass-loss rate of the source as $\dot{M} \approx m/\Delta\tau \approx (1\text{–}3) \times 10^{-7}\ M_\odot\ \mathrm{yr}^{-1}$.

It is interesting to note that equations (25) and (29) can be combined to give

$$\begin{aligned} L_{\mathrm{H}\alpha} &= \epsilon 2^{3-\kappa}\pi r_{\mathrm{jet}}^2\,\xi n_e kT v_s^{2\kappa-4}\left(\frac{\Delta\tau}{x_s}\right)^{\kappa-2} \\ &= 3.11 \times 10^{-7}\ L_\odot \left(\frac{r_{\mathrm{jet}}}{2\times 10^{15}\ \mathrm{cm}}\right)^2 \left(\frac{\xi}{10}\right) \\ &\times \left(\frac{n_e}{1000\ \mathrm{cm}^{-3}}\right)\left(\frac{T}{10^4\ \mathrm{K}}\right)\left(\frac{v_s}{200\ \mathrm{km\ s}^{-1}}\right)^{3.6} \\ &\times \left(\frac{\Delta\tau}{30\ \mathrm{yr}}\,\frac{1.5\times 10^{17}\ \mathrm{cm}}{x_s}\right)^{1.8}\ , \end{aligned} \tag{30}$$

where for the second equality we have again normalized the parameters to the values of the HH 34 jet (see § 2). This amounts to a prediction of the Hα luminosities of the knots of the HH 34 jet. Unfortunately, as far as we are aware no spectrophotometric measurements of such line fluxes have been carried out for this object.

7. THE MATTER LOST FROM THE JET FLOW

The internal working surfaces have the very important effect of "intercepting" gas from the jet flow (i.e., the gas that goes through the forward- or the backward-facing shocks, see Fig. 1). This gas is ejected sideways into the near environment, and will form a "cocoon" around the jet, with a possibly very complex structure. If the cooling distance behind the working surface shocks is smaller than the jet radius (see § 8), this cocoon will be cool, and in principle would be invisible in the optical atomic lines. In the following, we will estimate what fraction of the ejected mass ends up forming part of this cocoon.

In a steady state, the mass $\dot{m}$ ejected sideways (per unit time) by a working surface has to be equal to the mass intercepted by the forward- and backward-facing shocks (see Fig. 1). In other words

$$\dot{m} = \sigma\rho_1 v_1 + \sigma\rho_2 v_2 , \tag{31}$$

where σ is the cross section of the jet, and the preshock densities ρ_1, ρ_2, and shock velocities v_1, v_2 have been defined in § 4. Using equations (11), (19), and (31) we then obtain

$$\dot{m} = \frac{v_s^2 \Delta\tau}{x_s^2}(m_1 f_1 + m_2 f_2) = \frac{v_s^2 \Delta\tau}{x_s^2} m , \tag{32}$$

where for the second equality we have assumed that the source is periodic. This equation can be integrated over time in order to give the total mass $m_L(x_s)$ ejected (sideways, into the cocoon) by the working surface as it traveled from the source to the position x_s. However, as it is clear from equation (32), the integral diverges at the position of the source. This is a direct result of the fact that our theory for the motion of the working surfaces applies only for large distances from the source (see § 3). However, we can still carry out the integral and determine the integration constant by requiring that $m_L(x_s) \to M$ (where M is the total mass of an ejection event) for $x_s \to \infty$. However, as we have discussed in § 3.3, we have $M \sim m$ (i.e., for an outflow event the total mass is of the same order of magnitude as the characteristic mass). In this way we obtain

$$\frac{m_L(x_s)}{m} \approx 1 - \frac{\Delta\tau v_s}{x_s} , \tag{33}$$

where we have again considered the case of a jet from a source with a periodic time-variability. For the parameters of the HH 34 jet (see § 2), we obtain $m_L/m \sim 0.87$. In other words, 87% of the mass of the outflow is in the cocoon, and not in the jet itself. As we discuss in the conclusions, this result has very interesting implications.

One question that remains is whether or not the mass that has been "intercepted" by the working surfaces is actually ejected sideways into the cocoon. In principle, it is also possible that a substantial mass of gas might accumulate in the regions between the two shocks of the working surfaces (see Fig. 1).

The amount $m_{\rm trapped}$ of "trapped" matter of course depends on the velocity $v_{\rm out}$ at which the material is ejected sideways into the cocoon. Let us assume that $v_{\rm out} \sim c_s$, where c_s is the sound speed of the line-emitting region. Under this assumption, from the shock jump condition (eq. [26]) and general geometric considerations, we obtain

$$m_{\rm trapped} \approx \left(\frac{c_s}{\gamma v_{\rm shock}}\right)\pi r_{\rm jet}^3 \rho , \tag{34}$$

where ρ is the density of the gas trapped in between the two shocks of the working surfaces (i.e., the density of the line emitting region). For the parameters appropriate for HH 34 (see above and § 2), we obtain $m_{\rm trapped} \approx 5 \times 10^{-7}\ M_\odot$. From this, we would conclude that only a fraction $m_{\rm trapped}/m \sim 0.1$ (see eq. [29]) of the outflow mass remains in between the shock pairs of the working surfaces, and the rest of the mass intercepted by the shocks (eqs. [32] and [33]) is indeed ejected into the cocoon of the jet.

8. THE RADIATIVE COOLING IN THE WORKING SURFACES

In § 5, we have presented a simplified calculation of the Hα intensity of the internal working surfaces. For this calculation, we have assumed that the cooling distance $d_{\rm cool}$ behind the shocks (which are associated with the working surfaces, see Fig. 1) is smaller than the jet radius $r_{\rm jet}$. If this condition is met, the gas will cool before being ejected sideways into the cocoon, and the recombination region behind the working surface shocks can approximately be described with one-dimensional shock wave models.

Let us now try to see if for the conditions found in the HH 34 jet, the condition $d_{\rm cool} < r_{\rm jet}$ is indeed satisfied. We first determine the total (atom + ion) preshock density to be $n \approx 1300$ cm^{-3} (by evaluating eq. [27] with the parameters appropriate for HH 34, see § 2). If we then consider that the shocks in the knots of HH 34 have shock velocities $v_{\rm shock} \sim 20$ km s^{-1} (see § 4), we find that the cooling distance is $d_{\rm cool} \approx 10^{15}$ cm (where $d_{\rm cool}$ is defined as the distance from the shock at which the gas has cooled to a temperature of 10^4 K). This value of $d_{\rm cool}$ has been obtained by scaling to the appropriate preshock density the cooling distance for a 20 km s^{-1} shock calculated by Hartigan et al. (1987). As for the HH 34 jet we have $r_{\rm jet} \approx 2 \times 10^{15}$ cm, the $d_{\rm cool} < r_{\rm jet}$ condition is marginally satisfied.

In this way, we could conclude that the gas in principle does have time to cool before being ejected into the cocoon of the jet, and that our approximation of the working surface emission with one-dimensional shock wave models is approximately valid. We should note that for shock velocities $v_{\rm shock} \sim 20$ km s^{-1} the cooling distance increases most steeply with decreasing shock velocity (see Raga & Binette 1992). Because of this, the validity of our conclusion that the gas has time to cool before leaving the working surface hinges on the precise value chosen for the shock velocity. For example, some of the knots in the HH 34 jet could have somewhat lower shock velocities, in which case the observed emission (at least from some of the emission lines) might come from gas which is already in the cocoon of the jet. Without detailed two-dimensional hydrodynamic calculations, however, it is very hard to say what would be the observable effects of such a situation.

9. CONCLUSIONS

We have presented a model for jets from time-dependent sources, under the assumption that the flow has a high Mach number and a slowly varying cross section. We find that it is possible to find a general analytic solution valid for large distances from the source, that describes both the motion of the internal working surfaces (which are produced as a result of the time-variability of the source) and the flow field in between the successive knots.

From this solution it is possible to obtain very simple analytic relations giving the strength of the shock waves, the Hα luminosity, and the mass involved in the successive outflow events as a function of the observed parameters (position, knot spacing, velocity, electron density and temperature) of the knots of the jet. If we apply these relations to the parameters observed for the HH 34 jet, we conclude that the knots of this jet have associated shock velocities of $v_{\rm shock} \approx 10$–20 km s^{-1} (which is in qualitative agreement with the very low excitation spectrum of this object), that the Hα luminosity of each knot is $L_{\rm H\alpha} \sim 3 \times 10^{-7}\, L_\odot$ (which could be confirmed or not by future spectrophotometric observations of HH 34), and that the knots come from quasi-periodic outflow events with time periods $\Delta\tau \sim 20$–40 yr and characteristic masses $m \approx 7 \times 10^{-6}\, M_\odot$. We also conclude that the mass loss rate from the (time-dependent) outflow source of HH 34 should have an average value of $\dot{M} \approx (1$–$3) \times 10^{-7}\, M_\odot\, {\rm yr}^{-1}$.

The properties deduced for the source of the HH 34 jet have the following uncertainty. The source in principle might have a time-variability with substantially shorter characteristic time scales. Provided that the source variability is nonperiodic, the closely-spaced knots that would be produced could overtake each other and merge into brighter, higher shock velocity knots (this merging process is described by Kofman & Raga 1991). At large distances from the source, we would only observe such "merged knots," so that the time scales, energetics, etc., deduced from the observations of these knots might not correspond to the parameters of individual "ejection events" of the course.

We also find that if we assume that the knots of the jet are a result of a quasi-periodic oscillation of the source, the Hα intensities of the knots should decrease (at large distances from the source, where our analytic model is valid) as $x_s^{-4.8}$, where x_s is the distance measured from the source. Very surprisingly, we find that the knots farther away from the source of HH 34 do approximately follow such an intensity versus position trend. This could be interpreted as an indication that the knots of the HH 34 jet might indeed correspond to internal working surfaces in the jet flow. However, this interpretation of the knot structure of stellar jets needs further confirmation (tentative work in this direction has been recently carried out by Reipurth, Raga, & Heathcote 1992; and by Raga & Noriega-Crespo 1991).

Another interesting conclusion is that at the distance from the source at which we observe the bright knots of the HH 34 jet, already $\sim$90% of the mass of the outflow has been lost from the jet. This "mass loss" from the jet into the near environment (possibly forming a cool "cocoon" around the jet) occurs due to the fact that the internal working surfaces "intercept" gas from the jet flow, and eject it laterally into the near environment.

One would of course be tempted to think that these cool, massive envelopes of jets might in some way be related to the associated molecular outflows (see, e.g., the review of Cabrit 1989). However, in order to pursue this idea, one would have to understand (at least in a qualitative way) the interaction of the matter lost from the jet with the surrounding environment. This possibility should be addressed in future work.

A. R. would like to acknowledge Jorge Cantó, John Dyson, Sam Falle, and Franz Kahn for their insightful comments on this work, and John and Rita Dyson for their kind hospitality during his stay in the Astronomy Department of the University of Manchester. A. R.'s work was supported by an International Fellowship of the Natural Sciences and Engineering Research Council of Canada. L. K.'s work was partially supported by the Canadian Institute for Advanced Research. We would also like to thank John Raymond (the referee) for his helpful comments and J. Cantó, L. Binette, and N. Calvet for allowing us to use the diagram for Figure 1.

REFERENCES

Brugel, E. W., Böhm, K. H., & Mannery, E. 1981, ApJS, 47, 117
Bührke, T., Mundt, R., & Ray, T. P. 1988, A&A, 200, 99
Cabrit, S. 1989, in ESO Workshop on Low Mass Star Formation and Pre–Main-Sequence Objects, ed. B. Reipurth (Garching: ESO), 119
Hartigan, P., Raymond, J., & Hartmann, L. 1987, ApJ, 316, 323
Hartigan, P., Raymond, J., & Meaburn, J. 1990, ApJ, 362, 624
Hughes, P. A., ed. 1991, Beams and Jets in Astrophysics (Cambridge: Cambridge Univ. Press)
Kofman, L. & Raga, A. C. 1991, ApJ, submitted
Mundt, R. 1986, Canadian J. Phys., 64, 407
Raga, A. C., & Binette, L. 1991, Rev. Mexicana Astron. Af., submitted
Raga, A. C., Cantó, J., Binette, L., Calvet, N. 1990, ApJ, 364, 601
Raga, A. C., & Mateo, M. 1988, AJ, 95, 543
Raga, A. C., & Noriega-Crespo, A. 1991, Rev. Mexicana Astron. Af., submitted
Rees, M. J. 1978, MNRAS, 184, 61P
Reipurth, B. 1989, in ESO Workshop on Low Mass Star Formation and Pre–Main-Sequence Objects, ed. B. Reipurth (Garching: ESO), 247
Reipurth, B. Bally, J., Graham, J. A., Lane, A. P., & Zealey, W. J. 1986, A&A, 164, 51
Reipurth, B., Raga, A. C., & Heathcote, S. 1992, ApJ, submitted
Wilson, M. J. 1984, MNRAS, 209, 923